

Hanno H. Heller\* and Werner M. Dobrzynski\*\*

Abteilung Technische Akustik  
DFVLR, 3300 Braunschweig, GermanyAbstract

Airframe noise as a seemingly impenetrable barrier for the reduction of aircraft noise has attracted considerable interest since almost one decade. The initially rather poor knowledge about the relevant aeroacoustic phenomena has spurred intensive research with the objectives of (1) better understanding airframe-noise generation and radiation processes in order to improve prediction, and (2) exploring ways and means to lower airframe noise itself.

This paper surveys the development of airframe noise research and the present state-of-the-art. Approaches to airframe noise prediction through either the "total aircraft"- or the "aircraft-component"-method are discussed, whereby wing trailing-edge sources and landing-gear/wheelwell sources as the prime contributors to airframe noise receive a fairly extensive treatment. Both theoretical aspects of airframe noise and relevant experimental efforts, particularly those pertaining to gliders as test-vehicles and testbeds, resp. are described. Finally, some more speculative thoughts on possibilities to reduce airframe noise and on future research areas are offered.

1. Introduction

Advances in subsonic aircraft engine technologies over the past two decades have reduced aircraft noise to levels, where "airframe noise" becomes comparable to propulsive noise especially during landing approach, where thrust and hence engine noise levels are low. Airframe noise is a result of the aerodynamic interaction of the airflow with certain airframe components, the wing-slats and flaps, and the landing gears in particular. Airframe noise levels are surprisingly high and can reach overall values close to 90 or 100 dB for large aircraft flying overhead in their landing-approach configuration (Fig 1).

Airframe noise has been referred to as the "ultimate barrier" that stands in the way of lowering aircraft noise by 10 EPNdB below FAR Part-36 certification levels, as envisaged as a near term goal in the CARD-study (Ref 1). In fact, a recent total system study conducted by MBB (Ref 2) towards achieving 10 EPNdB below FAR Part-36 levels through advanced acoustic nacelle treatment of the Airbus revealed that such

a goal could not be attained since airframe noise levels were found to be only 9 EPNdB below certification levels. It was recognized then, that precise prediction of airframe noise in terms of levels and spectral characteristics was imperative, since even a slight overdesign of acoustic nacelle treatment may in consequence waste hundreds of thousands of dollars. Indeed, it is probably not too soon to begin studies on the reduction of airframe noise itself, if the potential of engine nacelle treatment is to be fully utilized and to ultimately achieve such long term goals as 15 or even 20 EPNdB below current certification levels.

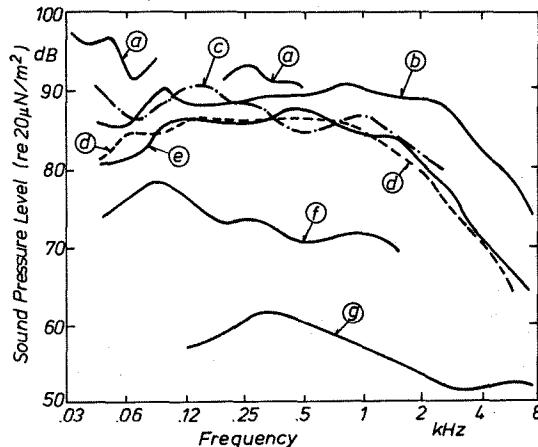


Figure 1 Airframe Noise ("Dirty Configuration Noise") of Several Aircraft, referenced to a Flight-speed of 100 m/s and Altitude of 100 m. (a) Galaxy C5A; (b) Boeing 747; (c) Vickers VC-10; (d) McDonnell Douglas DC-9; (e) Convair 990; (f) VFW 614; (g) SB-10 Glider

Thus airframe noise as a physical and ultimately technological problem has attracted considerable interest since about 1970, where airframe-noise was first recognized as a potential problem. A considerable amount of effort went into studies since that time towards a better understanding of the relevant aeroacoustic mechanisms, with the objective to first develop and then improve prediction techniques, and to provide guidelines towards lowering airframe noise below its present levels.

This paper surveys the development of airframe noise research and the present state-of-the-art as exemplified through the results of some recent study-programs.

\* Manager

\*\* Senior Scientist

## 2. Basic Concepts in Airframe Noise Research

In order to discuss concepts and approaches to airframe noise research, those aircraft components that are the most likely contributors of airframe noise need to be identified.

Fortunately - in a sense - there are only two of these, namely the wings and the undercarriage. Unfortunately, each of these components represents an extremely complex mechanical device with numerous potential acoustic "sub-contributors". Fig 2 shows an aircraft in the approach configuration. Wing leading-edge slats and wing trailing edge flaps are deployed, as well as the nose-, and several main landing gears. The landing-gear wheel-wells are - at least in part - open, and the wheel-well doors protrude into the external flow. Each component interacts with the external airstream in a complex manner, to constitute an aeroacoustic source of high complexity.



Figure 2 Large Commercial Aircraft during Landing Approach

Ideally, one would like to understand and then predict noise radiation from each of these components, considering them as sources that radiate sound independently of each other. The total airframe noise would then "simply" be the sum of the noise radiation from all individual sources. Unfortunately, these components do not act as independent sources, but interact in a sometimes very complex manner. For example, the unsteady wake flow shed from the landing-gear may impinge on the fully deployed flap-system, thus causing highly turbulent flow to interact with leading or trailing edges of flaps. Also, the unsteady flow-pattern in the wheel-wells, responsible for wheel-well noise generation is heavily affected by flow about the landing-gear struts. Thus, in studying airframe noise sources, there is a need to not only consider individual aircraft components, such as the wing, the slat- or flap-system, the landing-gear, the wheel-wells and the well-doors, but to investigate their aerodynamic and acoustic interaction. This is what makes airframe

noise such a complex phenomenon.

In the course of time two approaches to study and predict airframe noise have evolved, the *total aircraft method* and the *component method*, which includes the *drag-element method*, and the *distributed-source method*. The *total aircraft method* relates airframe noise radiation on a largely empirical basis to aircraft and flight parameters, such as gross weight, wing area, wing aspect ratio, and flight-speed. The *drag-element-method*, being somewhat more sophisticated, ties airframe noise to the steady-state-drag of aircraft components. Finally, the *distributed source method* employs - wherever possible - basic physical principles to characterize aeroacoustic generating and radiating mechanisms for as many individual airframe-noise-generating components of the aircraft as seem feasible. Here, the breakdown may go as far as to individual subcomponents of, say, the landing gear, e.g. its shafts, actuators, axles, wheels etc. In principle, the distributed source method should be the most accurate, since the noise source is separated into (hopefully) all of its constituents and basic aeroacoustic source mechanisms are used for predictive purposes. However, this method is also the least advanced due to the inherent complexity of the approach.

## 3. Airframe Noise Prediction through the Total Aircraft Method

The initial approach for the prediction of airframe noise was entirely empirical. Aircraft flyover noise data for aircraft in the cruise configuration with flaps and gears retracted and the engines as close to idle as (safely) possible served to derive empirical prediction schemes for overall noise and spectra. Later on aircraft were also studied in their "dirty" configuration, where either only flaps, or only gears, or both flaps and gears were deployed. Comparison studies were conducted with gliders but solely for the purpose of relating gross aircraft and operational parameters to radiated airframe noise. Table I is a fairly complete listing of those aircraft that were used since 1970 specifically in the context of airframe noise studies.

One of the first to offer a semiempirical prediction scheme for overall airframe noise was Healy (Ref 3), who used data from 5 propeller aircraft and one glider. The raw data as measured are shown in Fig 3, implying a general dependence of overall airframe noise on the 6th power of velocity. Healy applied a "spectral smoothing process" whereby he argued that non-uniformities in the spectra were due to potential vehicle sources such as antennas, pitot tubes, wheel-well-cavities, engine nacelles, feathered propellers and the like. Hence the idealized spectra would isolate those effects solely due to general aerodynamic noise, rather than being peculiar to any individual aircraft. After this operation overall

levels could be precisely predicted by equation (1) on Table II. This equation links overall sound pressure to the sixth power of velocity, to the wing area and, somewhat surprisingly, to the minus fourth power of the wing aspect ratio.

Likewise, a representative non-dimensional airframe noise spectrum was offered (Fig 4) on the basis of the "smoothed" spectra.

Using the same aircraft data and additional data obtained on a Galaxy C5A aircraft Gibson (Ref 4) came up with a slightly different prediction scheme, that relates overall sound pressure to the sixth power of velocity, the wing area and the minus first power of the aspect ratio, as shown by equation 2 on Table II. Both authors claim that predictions were found to

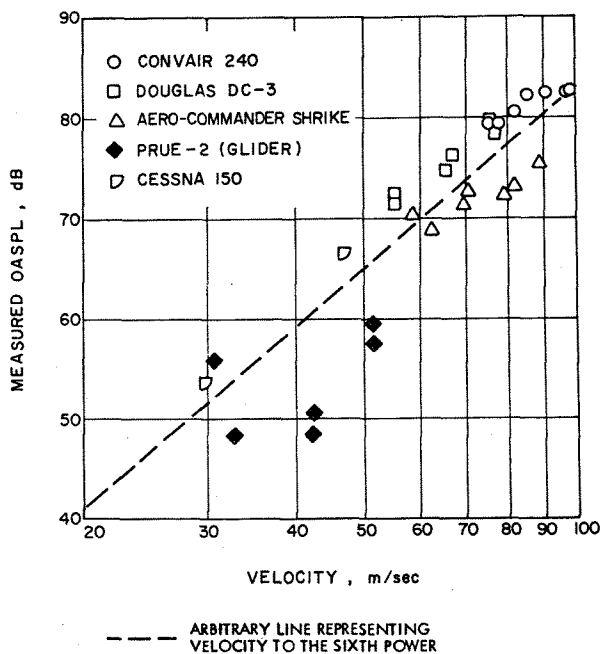


Figure 3 Overall Airframe Noise (including "parasitic" noise) of 5 Aircraft after Healy (Ref 3)

be accurate within a +1 and -1,5 dB range for moderate to high aspect ratio aircraft, while gross overpredictions were found, when applied to a supersonic delta-wing aircraft, flown in a gliding mode (Ref 5).

Hardin et al (Ref 6) using essentially Healy's data, and data from glider measurements as reported by Smith (Ref 7), as well as relevant information on 3 more aircraft (Aero-Commander, JetStar and F 106-B) employed a linear regression analysis to find best data collapse when sound pressure is taken as being proportional to the fifth power of velocity, the 3/4 power of wing area and the minus second power of aspect ratio (Equ 3 on Table II).

Yet a different scheme was offered by Putnam et al (Ref 8) who found good collapse

of airframe noise data from a JetStar, a F 106-B, a B 747, a CV 990, and the Prue glider on a simple velocity to the fifth power and direct weight proportionality (Equ 4 on Table II). However, since weight could be taken as lift, and lift being proportional to the square of the velocity, Putnam's method would actually imply a seventh power of velocity dependence for overall airframe noise.

Several similar or derived schemes were later developed and used to collapse data from one set of aircraft or another. For example Fethney (Ref 9) reports that overall levels from geometrically rather different aircraft (HP 115, HS 125, BAC 1-11, and VC-10) are not well predicted on the basis of Gibson's and/or Healy's formula indicating the non-transferability of prediction schemes to aircraft of radically different types and shapes. Fethney even suggests a slower variation of levels with flight speed, close to a fourth power of velocity dependence.

These few citations may illustrate the wide variety of possible prediction schemes available for the overall maximum sound pressure level directly below the flight-path. As an example for a somewhat definitive recent attempt to collapse essentially all available overall noise data through one simple prediction scheme, the work of Fink (Ref 10) should be mentioned, who plotted data for no less than 16 aircraft on the basis of either a simple fifth power of velocity and wing area basis, or, alternatively on a fifth power of velocity and a direct proportionality of wing trailing edge boundary layer thickness and wing span. The first of these two representations is shown in Fig 5, illustrating rather conclusively that no simple prediction scheme employing

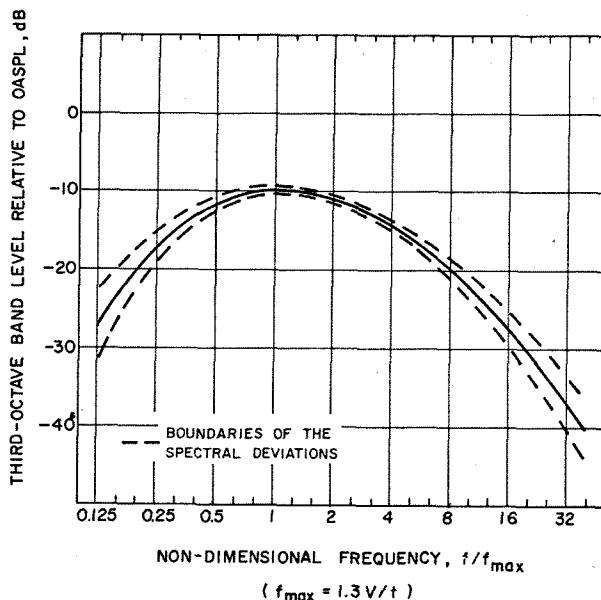


Figure 4 Non-dimensional Airframe Noise Spectrum after Healy (Ref 3)

gross aircraft and flight parameters can be

devised to collapse data from aircraft of widely differing types. To fit certain sets of data overall sound pressure need sometimes be related to either a fifth or a sixth power of velocity, sometimes to the wing surface area and sometimes not, and, most enigmatically to aspect ratios to the zeroth, the minus second or minus fourth power. All this variability indicates a highly unsatisfactory state of affairs.

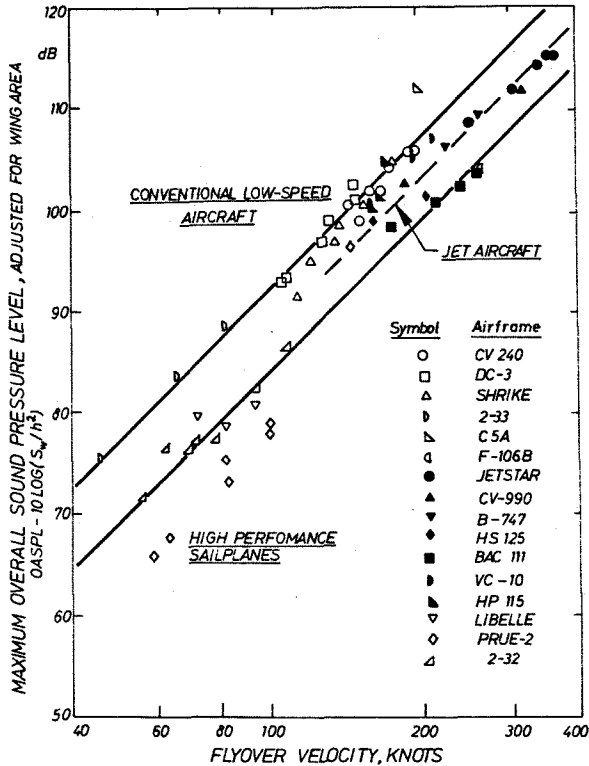


Figure 5 Overall Airframe Noise Data from 16 Aircraft after Fink (Ref 10)

May be, searching for the all-encompassing overall airframe noise prediction scheme is a futile endeavor, in particular when "dirty" aircraft configurations are to be considered. Fethney (Ref 9) on the example of the VC-10 shows how - in a rather unpredictable manner - radiated overall airframe noise changes with the successive deployment of flaps, slats, and landing gears (Fig 6). Obviously, the problem of predicting airframe noise for aircraft in the landing approach configuration cannot be tackled through just one simple additive quantity.

Thus, to increase confidence in airframe noise prediction methods there is a need to understand better both physically and mathematically the pertinent aeroacoustic mechanisms of each individual airframe-noise-producing aircraft component, as well as relevant interaction phenomena. The "component method" and pertinent theoretical and experimental efforts as described in section 4 provide the basis for such an improved understanding.

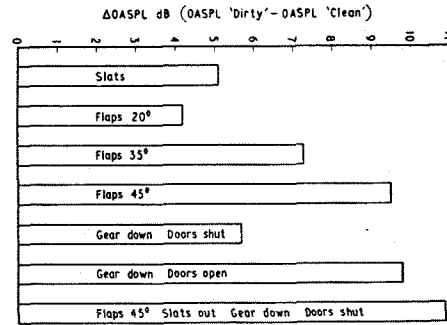


Figure 6 VC-10: Noise Increases due to Changes from the "Clean" Configuration with Engine Noise extracted (after Fethney, Ref 9)

#### 4. Airframe Noise Prediction through Component Methods

A more refined view, such as provided by either the *drag-element method* or by the *distributed-source method* is necessary to improve airframe noise prediction accuracy.

The drag-element method developed by Revell (Ref 11) is based on the hypothesis that sound generation by an object in flow can be related to the steady-state drag it experiences. The argument is advanced that the fluctuating aerodynamic drag which constitutes an aeroacoustic source mechanism is a function of steady-state drag. Revell utilizes three categories of drag for the various aircraft components, namely (a) wing profile drag, (b) induced drag or trailing vortex related drag, and (c) fuselage and other "parasitic" drag, claiming that any noise generating component of an aircraft can be associated with at least one of these drag forms. The potential advantage of the drag-element method is that it involves drag quantities which to any aircraft designer are more or less straight forwardly available.

The approach to airframe noise that is probably closest to the actual physical generating mechanisms, however, is the distributed-source analysis method, most advanced by Hayden (Ref 12). It requires positive identification of the individual noise generating aircraft components, and of the appropriate source mechanisms. From the basic understanding of the respective aeroacoustic source mechanism the source-spectrum of each mechanism and for each component resp., is predicted and its farfield contribution at some observer point determined, accounting for atmospheric propagation-, ground reflection-, and moving source effects.

Table III presents the aircraft components predominant in generating airframe noise together with the appropriate aeroacoustic mechanisms.

These mechanisms and the pertinent theoretical models will be described in the following section (4.1), while research and re-

sults on component studies pertaining to the wing and the landing-gear/wheel-well configurations, will be discussed in sections 4.2 and 4.3, resp.

#### 4.1 Theoretical Basis for Airframe Noise Prediction

Starting point for essentially all studies on the problems of sound generation by turbulent flows was Lighthill's "General Theory of Aerodynamic Sound" (Ref 13) formulated in the early fifties. Shortly thereafter, Curle (Ref 14) extended Lighthill's theory to account for the effect of solid boundaries upon the sound generation by turbulent flows. His work in essence represents the basis for sound generation through flow/solid-body interaction, and thus for the phenomenon of "airframe noise".

Curle shows a twofold effect of a solid boundary on the radiated sound by a turbulent flow field, namely

- reflection and diffraction of the sound waves at the solid boundaries,
- a resultant dipole field at the solid boundaries, which are the limits of Lighthill's quadrupole distribution.

Thus, Curle obtains a surface integral over the forces as the solution of the inhomogeneous wave equation, which are a result both of the effect of the sound waves of the Lighthill quadrupole sources and of the hydrodynamic forces as caused by the turbulent flows upon the surface. To determine the sound radiation by a body in flow, information on the spatial and time-dependent characteristics of these forces is necessary. This information, however, is usually not available, largely because of the presently rather incomplete understanding of turbulence structures. Thus, physically plausible simplifications and assumptions - depending on the particular case considered - are required to obtain approximate solutions. Quantitative information is attainable only on the basis of experimental data.

##### 4.1.1 Acoustically Compact Sources

On the basis of a dimensional analysis Curle developed a simple proportionality for the sound radiation by a body in flow, when body dimensions were small compared to the characteristic acoustic wave length

$$(1) \quad I \propto \frac{\rho_0 U^6 l^2}{a_0^3 r^2}$$

For the "simple" case of an acoustically compact source, the sound intensity is proportional to the sixth power of a characteristic flow velocity, and to the square of a characteristic body dimension. Thus, under the above mentioned constraints equ 1

could be applied to sound radiation by a bluff body in flow, such as a landing gear, or its components.

##### 4.1.2 Turbulent Flow on an Infinitely extended Surface

Rather more difficult is the mathematical treatment of sound generation by a turbulent surface-flow field on an infinitely extended surface. Early results by Philips (Ref 15) or Powell (Ref 16), for example, were of rather qualitative nature; however both indicated already that due to mutual cancellation of turbulent-pressure sources of neighboring areas, a turbulent boundary layer is not a very efficient sound radiator. More recently, Vecchino and Wily (Ref 17), Tam (Ref 18), and Pan (Ref 19), pointed out, that in the treatment of turbulent boundary layer noise, viscous forces and the compressibility of the fluid medium must be accounted for. Vecchino and Wily show that the turbulent surface-flow related sound field is composed of the Lighthill volume-integral over the quadrupole source distribution within the turbulent flow-field, and of a surface integral (given by Lotsch, Ref 20) over the dipole-source distribution on the surface; this dipole-source distribution can be determined from the surface pressure fluctuations, which are termed "pseudo-sound". Hence, the portion of the sound field due to quadrupole-sources is a function of  $U^8$ , while that due to the dipole sources obeys a  $U^6$  dependence,  $U$  being a typical flow-velocity.

##### 4.1.3 One-sided Flow on a Semi-infinite Surface

Two fundamentally different sound generating mechanisms for turbulent flow passing the edge of an otherwise infinitely extended surface have been developed.

Starting from Lighthill's quadrupole distribution in a turbulent surface boundary layer, Ffowks-Williams and Hall (Ref 21) show the *acoustic effect* of an edge within a turbulent flow-field. Accordingly, an edge acts as a "scattering center" for those pressure disturbances within the turbulent boundary layer that would "normally" not radiate. These pseudo-sound sources at the edge then become radiating sources. The sound intensity radiated by one eddy due to the scattering effect is given by

$$(2) \quad I \propto \frac{k^4 \rho_0 U^4 \alpha^2 V^2}{\pi^3 a_0^3 r^2 (kr_0)^3} \propto \rho_0 U_c^3 \left(\frac{U_c}{a_0}\right)^2 \cdot \frac{1}{r^2}$$

where  $U_c$  is the convection velocity of the eddy of typical dimension  $l$  (or of typical volume  $V$ ),  $\alpha$  is the turbulence intensity,  $r$  is the distance of source and observer, and  $r_0$  the distance of the "eddy-system" from the edge. Equ (2) shows that because of the factor  $(kr_0)^{-3}$  those eddies being closest to the edge generate the most intense sound. Di-

mensional analysis allows to express equ 2 in the form given on the right-hand side. This representation indicates the dependence of the radiated sound intensity on the fifth power of the convection velocity.

Ffowks-Williams gives the directivity of the radiated sound field in the plain parallel to the flow-direction and orthogonal to the edge as  $\cos^2(\frac{\theta}{2})$  where  $\theta = 0$  in the surface plain.

In contrast to this "edge-scattering model", Powell (Ref 16) and later Hayden (Ref 22) propose a *hydrodynamic* sound generating mechanism at the edge. The sudden pressure release at the edge is said to cause a momentum fluctuation at the edge, or, more precisely, just downstream of the edge. The hydrodynamic acceleration of fluid flow elements just downstream of the edge permits this process to be described by a distribution of dipole sources along the edge, which can be considered as acoustically compact, since the process occurs within "one correlation-length". Morse and Ingard (Ref 23) give the sound power of a simple (point-) dipole source as

$$(3) \quad \pi_0(\omega) = \frac{3}{4} \frac{\omega^2 F^2(\omega)}{\pi \rho_0 a_0^3} \quad \text{for } kl \ll 1,$$

where  $F(\omega)$  is taken as the force required to accelerate a fluid element of dimension  $l$ .

Through dimensional arguments Hayden takes this force to be proportional to the product of the free-stream dynamic pressure and a correlation area of dimension  $l_x$  in the streamwise and  $l_y$  in the lateral direction. Since both these correlation lengths themselves relate to the ratio of a characteristic velocity and a characteristic frequency, he finally determines the sound power radiation from the edge of length  $Y$  as

$$(4) \quad \pi_{\text{total}} \propto \frac{3\pi \rho_0 U^6 l_y Y}{4 a_0^3}$$

In contrast to the Ffowks-Williams and Hall edge scattering model which leads to a  $U^5$  dependence, equ 4 yields a  $U^6$ -dependence of the sound power. In analogy to Ffowks-Williams and Hall's model, Hayden also finds a directivity corresponding to  $\cos^2(\frac{\theta}{2})$  for the case considered of flow past the edge of an semi-infinitely extended plain. Hayden calls this source a "half baffled dipole".

In a more recent paper of Hayden et al (Ref 24), the "hydrodynamic model" is refined by not only accounting for the average or mean fluid flow quantities (the flow velocity in particular) but also for the turbulence properties of the surface flow (turbulence-isotropy and scale in particu-

lar). This more sophisticated model leads to a dependence of the velocity-exponent on Mach-number. The  $U^6$ -law is now considered the low-Mach-number limit, while for higher Mach-numbers, the velocity exponent decreases, depending on the turbulence properties.

## 4.2 Wing Trailing Edge Noise

### 4.2.1 Source Considerations

Applying the hydrodynamic edge noise model, as described in section 4.1, the far-field radiated sound from wing trailing edges can be predicted from the fluctuating surface characteristics in the vicinity of the edge. Unsteady forces resulting from unsteady fluid-element acceleration cause (equal and opposite) reactive forces on the trailing edge, where such forces could be measured in terms of fluctuating pressures acting on appropriate surface areas of correlation. It should be kept in mind that not the fluctuating surface forces on the trailing edge generate sound, but rather the unsteady hydrodynamic processes just downstream of the trailing edge, which are in turn - intimately related to the phenomena on the trailing edge.

On the basis of these considerations an analytical expression can be developed on the relationship of surface pressure spectrum and farfield radiated sound pressure spectrum: Assuming spherical radiation and replacing the force-term by the product of a surface pressure and a correlation area of extent  $l_x$  in the streamwise and  $l_y$  in the spanwise direction equ (3) can be rewritten as

$$(5) \quad \frac{P_F^2(f)}{P_S^2(f)} = \frac{9}{4} \frac{f^2 [l_x(f) l_y(f)]^2}{a^2 r^2}$$

providing the ratio of mean square farfield and surface pressure for one source element.

Thus, in order to compute the farfield sound radiation from the edge-located sources, the surface pressure spectrum representative for the source area must be known together with the spatial extent of the source element. For realistic wing-flows this information is not available.

Therefore, an experimental research program was initiated about 2 years ago by DFVLR (Ref 25), in order to determine under realistic conditions surface pressure spectra and pressure field correlation characteristics on an aircraft-wing. The test-aircraft was an aerodynamically very clean glider, which - in a sense - could be considered as a "near full-scale" equivalent when compared to typical medium-size commercial aircraft. Thus, fairly close to full-scale Reynolds-numbers for wing surface flows could be obtained. Since both source characteristics (i.e. trailing-edge unsteady flows) and farfield sound signa-

tures could be measured, this program served to check the relevance of trailing edge sources to the phenomenon of airframe noise.

#### 4.2.2 Prediction of Glider-wing Trailing-edge Noise from Surface Pressure Characteristics

The test glider - the Braunschweig Akaflieg SB-10 - is a high performance glider with an unusually large wing span of 29 m, and an average wing chord of 0.8 m, corresponding to a wing aspect ratio of 36.6. The wing profile pertains to the Wortmann-Series with classification FX 62135. At a flight speed of 50 m/s, the chord-based Reynolds-number is about 3.3 million. Within the speed range investigated flow transition occurs at the 50 to 60% chord position. Thus surface flow is fully turbulent under all flight conditions by the time it reaches the trailing edge. Surface pressure spectra were measured by flush mounted sensors near the trailing edge of the wing-flap, arranged both along and across the flow direction. Data were acquired at flight speeds up to nearly 60 m/s and for flap-settings from  $-10^\circ$  to  $+85^\circ$ , thus covering a range of typical cruise and landing approach conditions and configurations, resp.

Farfield noise radiation from the SB-10 was measured by condenser microphones laid flat on the concrete surface of the runway or alternatively elevated 5 m above ground to facilitate correction for reflection effects. Flight altitude and speed were determined from the ground through a high speed camera. Fig 7 shows the test aircraft above the measuring station.



Figure 7 Test Glider above Measuring Station

#### (a) Fluctuating Surface Pressure Data

Fig 8 shows typical surface pressure spectra just upstream of the trailing edge at a flap angle of  $\eta = 0^\circ$ . Surface pressures are normalized with the free-stream dynamic pressure, frequencies are non-dimensionalized on a Strouhal-number basis. The measured trailing-edge spectra (with the exception of the maximum near  $f \cdot \delta^*/U_\infty = 1.2$  which may indicate the presence of a discrete-frequency flow-shedding phenomenon at the trailing edge, to be discussed) correspond to those that have been measured for attached turbulent boundary layers with equal physical properties (i.e. displacement thickness, Reynolds-number). Hence the presence of a boundary discontinuity seems not to affect the properties of the approaching boundary layer flow which are in their entirety determined by the upstream flow history. The edge - of course - is instrumental in the sound

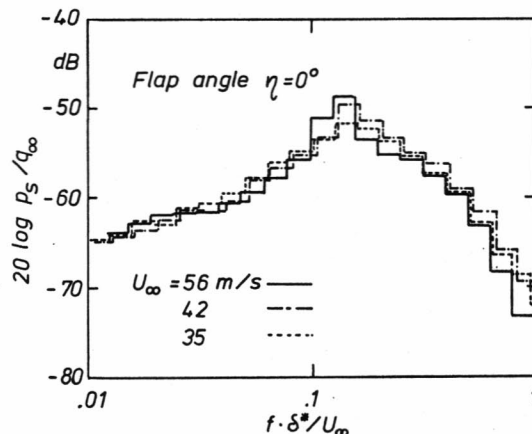


Figure 8 Typical normalized Wing-flap Trailing-edge Surface Pressure Spectra measured on the SB-10 Glider (not corrected for Finite Transducer Size)

generating process, leading to an aeroacoustic dipole mechanism due to flow-spillage past an edge.

Narrowband spectral analysis of trailing edge pressure fluctuations confirm the presence of discrete-frequency flow phenomena and indicate strongly periodic shedding processes even for turbulent boundary layer conditions. Evidently the phenomenon is localized at the very trailing edge, since upstream measurements do not show any periodic flow-behavior (Fig 9). Tones in the spectra cannot be normalized on a Strouhal-number basis with the displacement thickness as length-parameter. However, they were observed consistently and most pronounced for negative (i.e. upward) flap settings in the immediate vicinity of the trailing edge. Further upstream, as also observed by Hahn (Ref 26), the tones were immersed in the broadband noise level.

The typical data scatter that occurred for nominally identical flight conditions

(i.e.  $\pm 0.5$  dB) and, more pronounced, even for different sensor positions in the spanwise direction (i.e.  $\pm 2$  dB) is illustrated in Fig 10. Data for flap-settings of  $40^\circ < \eta < 85^\circ$  fall in a  $\pm 3$  dB band, with levels some 25 dB higher than for the low-angle flap-settings. The flow in all likelihood was fully separated for the larger flap deflections.

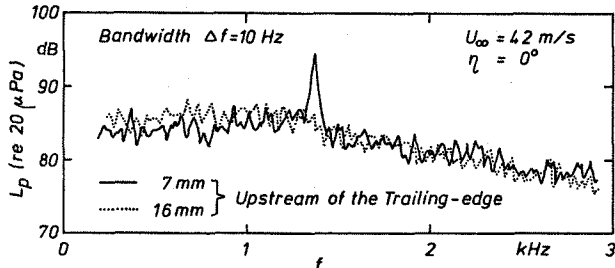


Figure 9 Narrowband Wing-flap Surface Pressure Spectra measured at two Locations upstream of the Trailing-edge (Flap Angle  $\eta = 0^\circ$ )

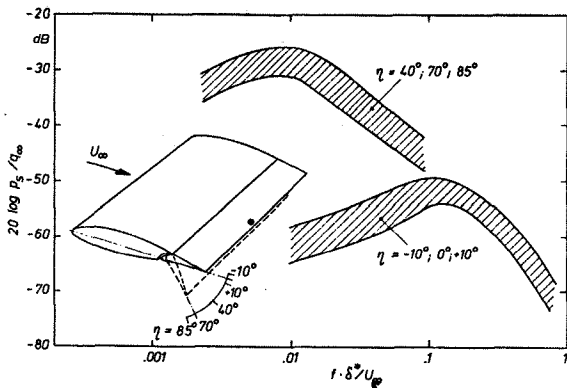


Figure 10 Wing-flap Trailing-edge Surface Pressure Spectra for different Flap Angles (not corrected for Finite Transducer Size)

(b) Pressure-field Correlation Characteristics

Fig 11 shows the longitudinal pressure field correlation in terms of a coherence  $\gamma$  versus a normalized sensor distance  $\Delta x / \delta^*$  as measured by Panton (Ref 27) on a flat portion of a glider fuselage. The coherence of the fluctuating pressures increases steadily towards unity with decreasing sensor-separation distance, but for a given sensor-separation distance, the coherence reaches a maximum at some frequency. Thus, a limiting frequency should exist below which no correlation length can be defined by integrating the curves shown in Fig 11.

Before determining this limiting frequency, Panton's data, together with data obtained in the DFVLR study (Ref 25) and data by Schloemer (Ref 28) and by Bull (Ref 29) are shown in a representation employing a

linear abscissa scale (Fig 12). The data need not necessarily fall all upon one curve since Panton's data were taken on a flat portion of a glider fuselage, while both

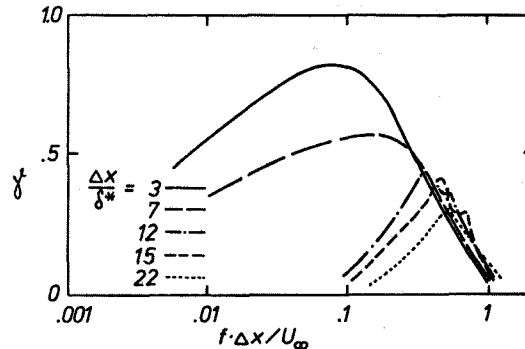


Figure 11 Longitudinal Coherence of Surface Pressure Fluctuations as Function of Normalized Sensor Distance measured on a Glider Fuselage (after Panton, Ref 27)

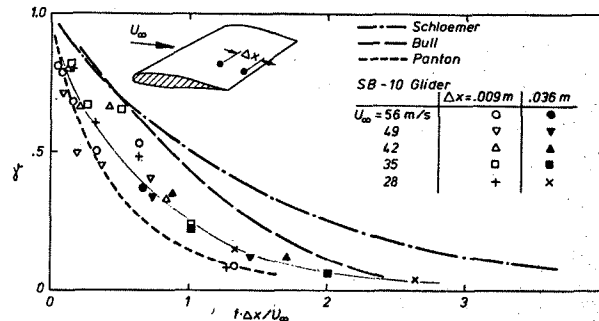


Figure 12 Longitudinal Coherence of Surface Pressure Fluctuations as Function of Normalized Sensor Distance

Schloemer and Bull obtained their data in windtunnels on straight surfaces. Since "coherence versus normalized sensor-separation distance" is a continuous function, correlation lengths can only be defined by a mean value, i.e. the integral of  $\gamma$  versus  $f \cdot \Delta x / U_\infty$ . Numerical integration of the curve drawn through the glider wing-flap data yields a longitudinal correlation length of  $l_x = 0.72 U_\infty / f$ . Corresponding information on the lateral coherence yields a correlation length of  $l_y = 0.26 U_\infty / f$ .

From Fig 11 it can be seen that the curves tend to collapse at frequencies above the frequency of the maximum coherence, but fan out at lower frequencies. Evidently, the limiting nondimensional frequency is given by that frequency where each curve branches off. The corresponding non-dimensional frequencies taken from data obtained by Panton (Ref 27), Bull (Ref 29) and also by Bhat (Ref 30), who measured longitudinal pressure field coherence on a B 737 aircraft fuselage, are plotted in Fig 13 both for longitudinal and lateral coherence. A straight line of unity slope can be drawn through the



data points, yielding a simple expression for the limiting frequency for both longitudinal and lateral correlation lengths of  $f_{limit} \approx 0.04 U_{\infty} / \delta^*$ . Hence, the above derived longitudinal and lateral correlation lengths are only valid for frequencies above those defined by the limiting frequency.

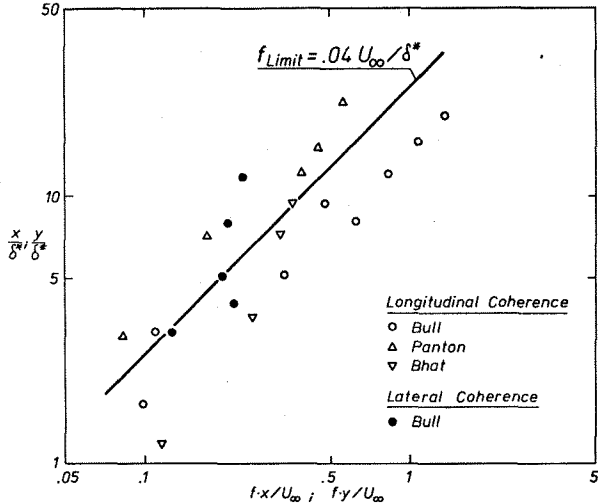


Figure 13 Relationship between the Frequency limiting the Normalization of Pressure Field Coherence Functions and the Corresponding Flow Parameters

(c) Farfield Sound Prediction

Having available all required input quantities, the validity of equation (5) can be checked. The following two suppositions were made: (i) The total radiating trailing edge area is represented by  $n = Y/l_y$  incoherently radiating areas along the trailing edge\* of extent  $l_x = 0.72 U_{\infty} / f$  and  $l_y = 0.26 U_{\infty} / f$ , in the streamwise and lateral direction, respectively, and (ii) the directivity of the source is that of a half-baffled dipole source.

Fig 14 shows acceptable agreement between predicted and measured spectra for the glider directly above the microphone. The high frequency peak in the measured spectrum near 3 kHz is most likely due to sound radiation from the horizontal stabilizer. Alternatively, it could very well be due to some periodic vortex-shedding off the trailing edge as had been observed for certain sensor locations near the flap trailing edge. The underprediction of the spectral portions above 4 kHz could be accounted for by applying a finite transducer

\* Distributing sound sources of equal strengths all along the trailing edge seems appropriate because of the large aspect ratio of the SB-10 glider wings; the wings in this context can be considered as being essentially "two-dimensional".

size correction (Ref 31).

4.3 Landing-gear/Wheel-well Noise

4.3.1 Review of Prediction Schemes

The treatment of undercarriage noise is frequently separated into that from the actual landing-gear, and that from the wheel-well. Treating the landing gear as an individual source is not necessarily wrong, since over most of the approach phase, the wheel-well doors are partly closed.

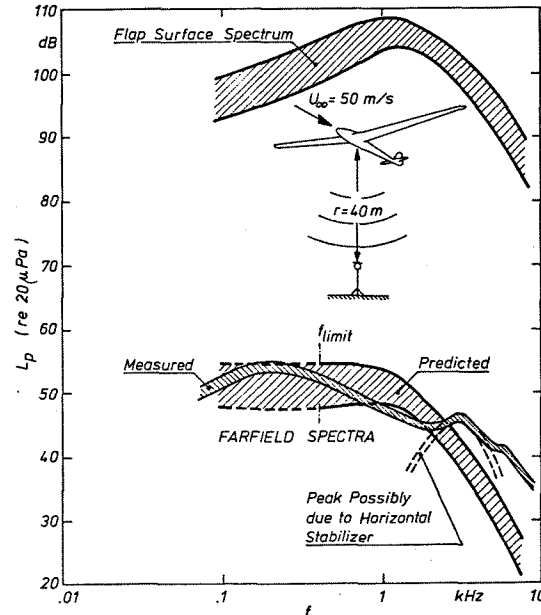


Figure 14 Prediction of the Farfield Sound Signature from Surface Pressure Characteristics on the SB-10 Wing-flap Trailing Edge

Both nose and main landing gears consist of many components, such as wheels, axles, shafts with lateral support struts, drag braces and actuators. All exposed subcomponents are essentially bluff bodies, inherently shedding unsteady wakes. From the scale of major landing gear components it is obvious that fairly low-frequency wake shedding phenomena will occur; hence, corresponding sound phenomena are of predominantly low-frequency character. On the other hand, small-scale structural elements such as wires, hoses, screw-holes, small-diameter cylindrical struts, etc., are likely to generate high-frequency noise. Thus, one would expect a fairly broad frequency spectrum to be emitted from a landing gear.

Hersh (Ref 32) considers a landing gear simply as one large dipole source and on that basis derives a prediction scheme that utilizes the induced drag on the landing gear when the gear geometry is idealized by either a "horizontal" cylinder of wheel-diameter and length corresponding to the overall wheel-distance, or, alternatively by a

"vertical" cylinder that has the diameter of the wheel distance and the protruding length of the entire gear. For one aircraft, the JetStar, where data was available for a "retracted flap, extended gear"-configuration, he evaluates a proportionality constant that related overall intensity to appropriate aerodynamic parameters such as steady-state drag-coefficient and the flow velocity, obtaining good overall landing-gear noise prediction also for the Convair 990 and the Boeing 747.

In an attempt to predict not only overall levels of landing gear configurations, but the spectral distribution of radiated energy too, Bliss and Hayden (Ref 33) subdivide a landing gear into its components and consider each of these as a bluff body which experiences fluctuating forces through the shedding of an unsteady wake. Depending on Reynolds-number and the particular geometry involved, this shedding process is either periodic or random and produces sound accordingly, i.e. tonal or broadband. In order to apply Curle's dipole formulation, for acoustically compact sources they take typical ratios of fluctuating and steady-state drag, as established by Heller and Widnall (Ref 34) together with a fluctuating force spectrum for certain kinds of bluff bodies, to determine a composite spectrum from a complicated body such as a landing gear.

In an effort to quantify the relevant acoustic phenomena and put predictions on a firmer ground the DFVLR initiated an experimental/analytical research program on landing gear/wheel-well noise (Ref 35).

First studies involved scaled replicas of both nose gear and main-gear configurations. Fig 15 and 16 show full scale nose landing gears and model configurations in comparison.

Such models were tested on a stationary wall-jet flow facility which had the advantage of easy model access, and provided the option to disassemble the model for component and interaction studies. Similar studies employing wind-tunnels were conducted by NASA-Langley (Ref 36) and are presently planned by Fink (Ref 37).

Acoustic data for a two-wheel landing-gear model configuration are shown in Fig 17 in a normalized fashion allowing straight forward extrapolation to a full-scale situation. Employment of these results to one particular aircraft with three two-wheel bogies (Lockheed JetStar) yields rather acceptable agreement (Fig 18). A similar approach employing four-wheel bogie model data to predict full-scale landing gear noise, however, shows rather poor agreement (Fig 19) namely overprediction for low-, and underprediction for high frequencies.

Based on some available full-scale data Fink (Ref 10) uses a curve-fitting approach to derive a landing gear aerodynamic noise

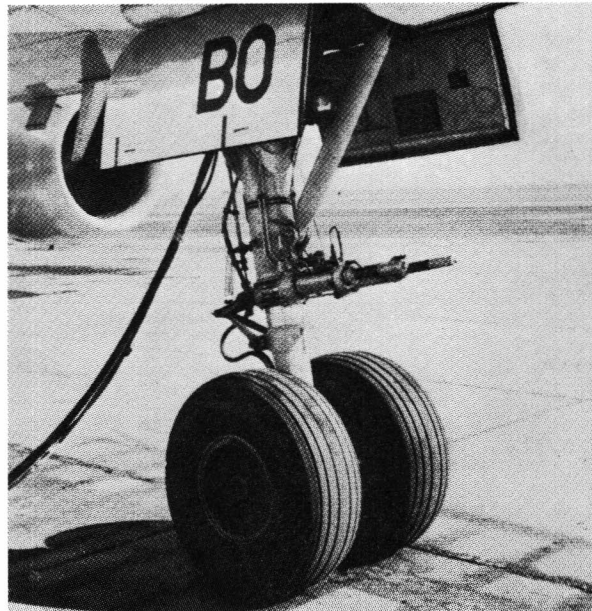


Figure 15 DC-10 Nose Landing Gear

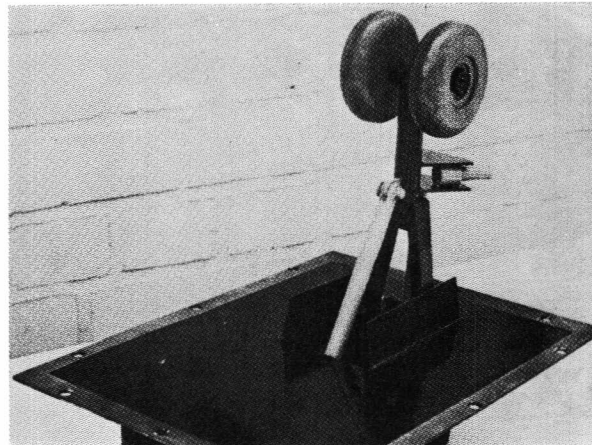


Figure 16 Nose Landing Gear Model

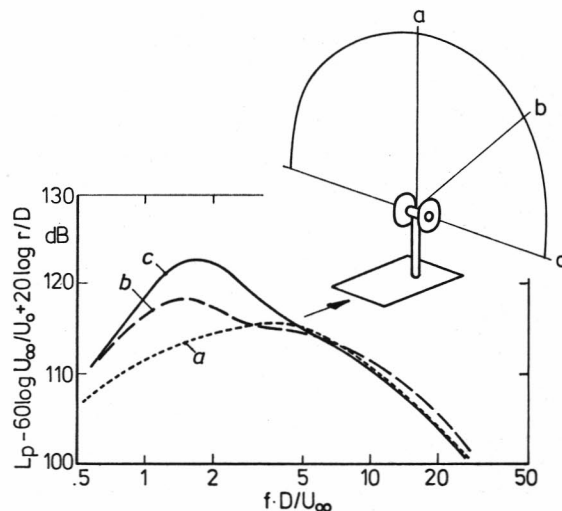


Figure 17 Normalized Nose Gear Model Spectra at 3 Measurement Points ( $U_0 = 100 \text{ m/s}$ )

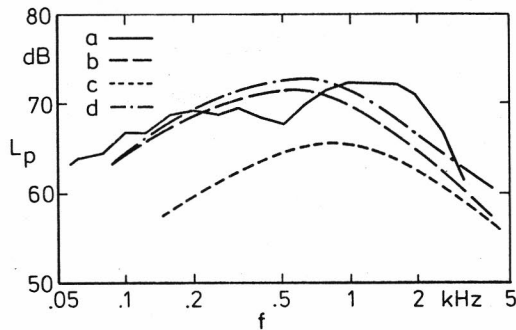


Figure 18 Comparison of Predicted and Measured Landing Gear Noise:  
 a = Measured Full-scale Data;  
 b = Predicted 2 Nose Gears;  
 c = Predicted 1 Nose Gear;  
 d = Sum of b and c  
 (Lockheed JetStar: Flight alt. 152 m; Flight Speed 103 m/s)

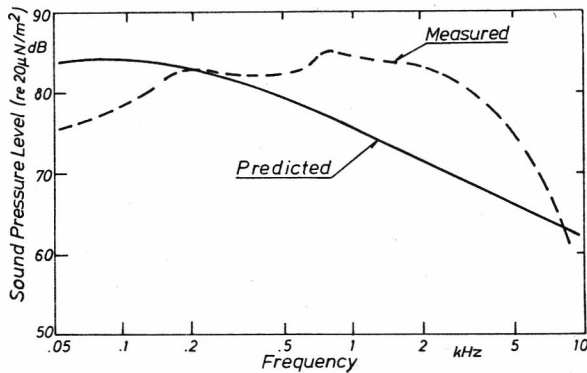


Figure 19 Comparison of Predicted and Measured 4-Wheel Landing Gear Noise (Boeing 747)

prediction scheme, which compared with full-scale data inherently provides excellent agreement, although no physical basis is provided in the context of this straight-forward approach.

From a more general point of view, then, it must be stated that extreme caution has to be applied in employing aerodynamic scaling to such a complex case as represented by landing gears, and that neither model scale experiments, nor calculation from basic (physical) principles provides the needed accuracy. Apparently Reynolds-number effects play a dominant role in aerodynamic scaling of landing gear aeroacoustic data.

#### 4.3.2 Prediction of Landing-gear Noise from Surface Pressure Characteristics

The understanding of the physical mechanisms involved in 4-wheel landing gear noise generation and -radiation has been furthered through model experiments, where flying test beds were employed.

An appropriate study that attempted to relate fluctuating surface pressure characteristics on 4-wheel gear models to radiated

noise is reported in Ref 35. Within this study two four-wheel landing gear models with a wheel diameter of .27 m were attached to the wings of the SB-10 airplane, thus employing a glider as "flying" test-bed (Fig 20). At typical glider flight speeds, Reynolds-numbers based on wheel-diameter were of the order of one million leading to turbulent flow separation even when the forward wheel set was impinged upon by undisturbed flow.

Four miniature piezoelectric sensors - two in a front wheel at both sides, two more in an aft wheel again at both sides - were installed flush within the surrounding surface in areas where particularly high fluctuating pressure intensities might act as potent sound sources.

#### (a) Fluctuating Surface-pressure Data

Previous model tests (Ref 38) have shown that the dominant mechanism responsible for sound radiation from a four-wheel main landing gear bogie is related to turbulent flow impingement on the rear set of wheels. In-

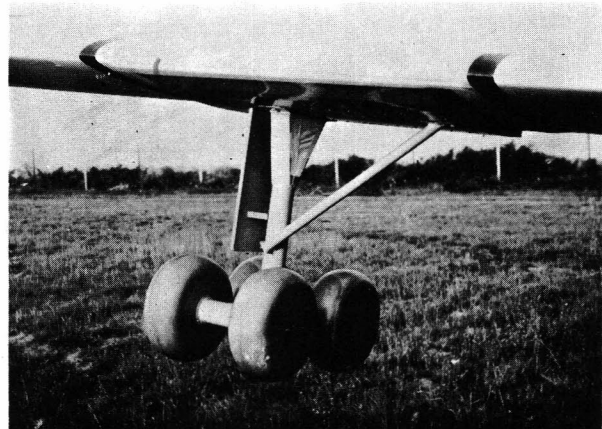


Figure 20 Four-wheel Landing Gear Model on Glider Wing

specting the flow pattern (Fig 21) it becomes quite obvious, why strong unsteady flow phenomena would occur at these locations: The turbulent wheel-flow wake is pushed downwards and inwards, resulting in violent flow patterns on the inside rear wheel with highest fluctuating pressures at these locations.

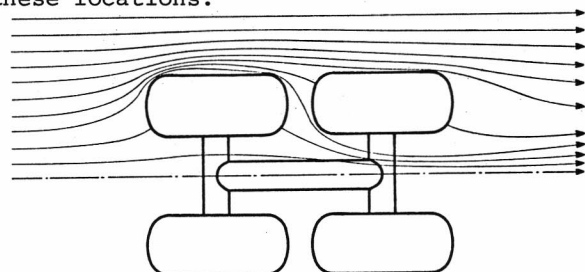


Figure 21 Schematic Flow Pattern around a Main Landing Gear Configuration

Surface-pressure spectra measured on the inside of the rear-wheel of the landing-gear model is shown in Fig 22. The data are normalized on a  $p_s/q_\infty$  versus Strouhal-number basis, with the wheel-diameter as the relevant length dimension.

(b) Source Considerations

While sound radiation from a wing trailing edge can be considered to be the result of "two-dimensional" flow phenomena, a landing gear causes the flow to assume complicated three-dimensional patterns. Thus the typical acoustic wavelength and the hydrodynamic wavelength at frequencies near the spectral maximum are both of the order of the body (i.e. landing gear) dimensions. In this regime, one would expect "whole-body-dipole" sound radiation.

The fluctuating pressures, measured on the wheels - as shown in Fig 22 - should thus not be considered representative for "isolated patches" on the gear, but rather as representative for the entire bluff body (specifically the rear set of wheels and axles). Large correlated turbulent regions shed from the forward wheel-set cause reactive forces to occur on the rear set of wheels of order  $p_s \cdot A$ , where  $p_s$  is the measured surface fluctuating pressure and  $A$  is a representative correlated surface pressure area on the wheel surface, responsible for the radiation of sound.

(c) Farfield Sound Prediction

In order to relate surface spectra to radiated farfield pressure spectra the same basic approach as used in the prediction of

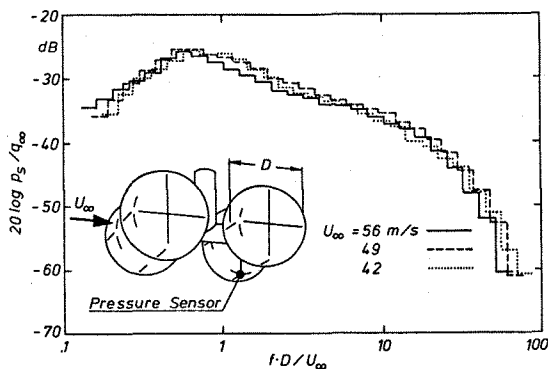


Figure 22 Typical Normalized Landing Gear Wheel-Surface Pressure Spectra

trailing edge noise was applied in this aerodynamically complex case, somewhat arbitrarily taking for both the lateral and longitudinal correlation lengths a value of  $l_x = l_y = 0.5 U_\infty / f$ .

Assuming the prime radiating area to be the inner portions of the rear treads where surface spectra were measured, a farfield spectrum was predicted and compared with a measured one (Fig 23). The agreement of pre-

dicted and measured spectrum is surprisingly good. It should be emphasized that the somewhat arbitrary assumption of the correlation lengths does not have much effect on the prediction.

Applying the appropriate analytical expression, one finds that in the high frequency region, farfield and surface pressure spectra have a  $f^0$ -dependence (i.e. their shapes are identical). At a frequency where the lateral correlation length becomes equal to half the width of the wheel, one finds a  $f^1$ -dependence.

Finally where the longitudinal correlation length becomes equal to that portion of the circumferential length - which is considered as radiating - a  $f^2$ -dependence.

The overprediction for high frequencies, where correlation lengths become small with respect to the body dimensions, might be due to cancellation effects of areas of correlated pressure fluctuations, an effect similar to infinite-surface boundary layer flow conditions.

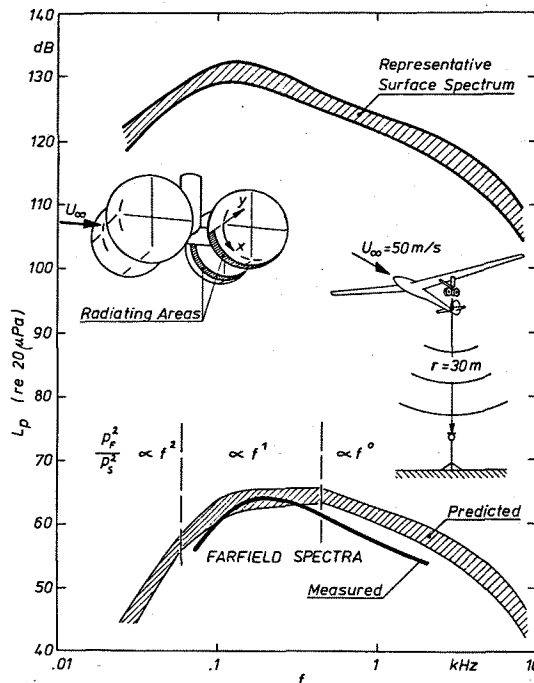


Figure 23 Prediction of the Farfield Sound Signature from Surface Pressure Characteristics on Landing Gear Aft Wheels

4.3.3 Wheel-well Related Airframe Noise

Cut-outs or cavities in aircraft structural surfaces that are exposed to high-speed external flow can give rise to intense pressure fluctuations, and in consequence to the radiation of intense tonal sound (Ref 39). Therefore, for many years it was thought that aircraft wheel-wells were to constitute important airframe-noise

sources. Although the treatment of "isolated" landing gears as a source of airframe noise is quite in order, treatment of "isolated" wheel-wells, however, is a purely academic exercise, because aircraft wheel-wells are invariably cluttered with gear components and are not "clean and empty" as would be a prerequisite for the generation of sufficiently intense "cavity-pressure oscillations".

Recently a definite experiment was conducted (Ref 35), that showed wheel-well pressure oscillations not to be an important airframe noise source. This experiment was conducted on a DC-10 Series 30 aircraft where microphones were positioned within the wheel-wells of (1) the nose gear, (2) the center-main gear, and (3) one side-main gear (Fig 24). The aircraft was then flown in the approach configuration with gears deployed and wheel-well doors open over a speedrange that corresponded to typical approach speeds up to twice that amount. The internal pressure response of the Center Main Landing Gear for example, analyzed in 1 Hz bandwidth at speeds of 77 and 151 m/s, shows no truly pronounced discrete tones in the frequency range from 0 to 300 Hz where such tones according to the wheel-well dimensions should occur (Fig 25). Furthermore, the well-internal pressure levels although high in an absolute sense are rather low from the view point of a farfield radiating airframe noise source. This conclusion was reached on the basis of appropriate model experiments.

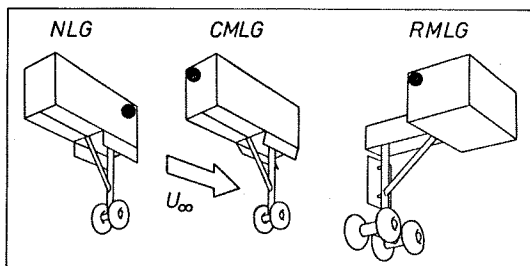


Figure 24 Schematic Representation of Microphone Location in the DC-10 Wheel-wells

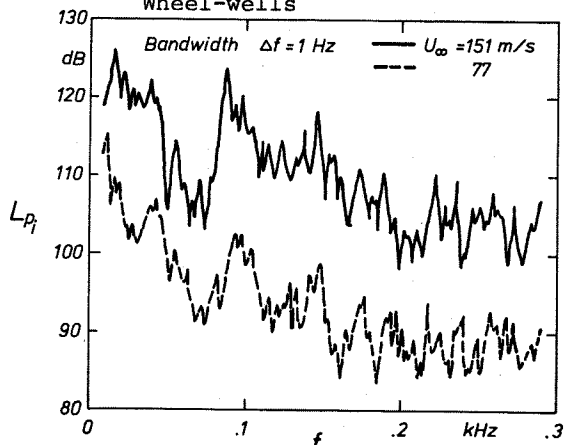


Figure 25 Effect of Flow-speed on DC-10 Center-Main-Landing-Gear Wheel-well Internal Pressure Response

A comparison of a measured landing gear related airframe noise signature for the VC-10 aircraft and of tones as predicted for the corresponding wheel-wells (Ref 35) reveal that the latter ones are unimportant (Fig 26).

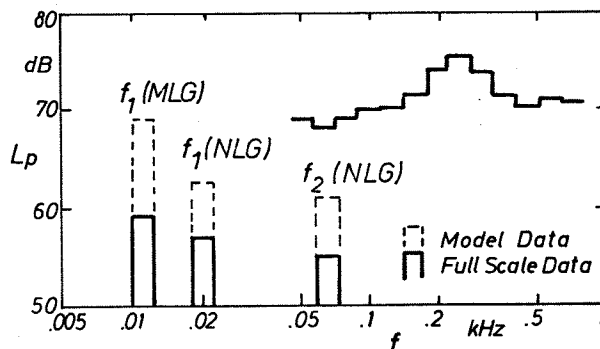


Figure 26 Comparison of Predicted Farfield Signatures of Wheel-well Resonances and Total Airframe Spectrum for VC-10 Aircraft at 183 m Altitude and 82 m/s Flight Speed

### 5. Noise Reduction Concepts

Since airframe noise cannot be controlled through either enclosing the various relevant sources, or applying sound-absorptive treatment to the radiating surfaces, which - in the case of the wings and/or flaps - would most likely jeopardize their primary purpose, only direct control of the generating and - if possible - radiating mechanisms offers possibilities to "trespass the ultimate barrier".

As far as the wings - as one of the primary airframe noise contributors - is concerned, a reduction in surface flow (i.e. flight-)speed would be most desirable. Since a direct reduction of flight-speed is however not feasible, one could reduce the local flow speed at, say, the wing and/or flap-trailing edges. This could be achieved through shaping the edge in a saw-tooth fashion (Ref 46), which would have an effect similar to that on swept-wing-edges of delta-wing aircraft. However, possible beneficial effects would probably be offset through the increased trailing-edge length.

Model tests have also shown, that edge-blowing could effectively decrease edge-noise generation. Here, comparatively very small amounts of secondary (bleed-)air, released just upstream of the trailing-edge have been found to reduce sound intensities (Ref 47). A similar effect could probably be achieved through a simple "comb-like" structure at the very trailing-edge with perhaps rather devastating companion effects on the lift. Hayden et al (Ref 48) conducted extensive experiments with - as he termed it - the "variable impedance edge": A porous edge extension results in a more gradual impedance change from the solid lifting

surface to the impedance of the surrounding air, with reportedly very beneficial results due to reduced fluctuating-force intensities. This concept could also be applied to the leading edges of flaps, or flap-systems. A decrease in turbulence scale of flow impinging on leading edges would also reduce sound intensities, or, at least, shift sound generation towards higher frequencies, which as the case might be could lower noise in a sensitive frequency range.

Prevention of large-scale turbulent eddies to occur at flap-trailing edges through operational means, e.g. flying with the smallest possible flap-deflection angle, should likewise be beneficial. As far as the landing-gear/wheel-well configuration is concerned, prevention of uniform (correlated) vortex-shedding from the various bluff constituents of a gear would reduce force fluctuations and - in consequence - radiation of sound. For the case of cylindrical struts, for example, Sallett (Ref 49) demonstrated the feasibility of using splitter-plates behind such bodies to suppress periodic flow-shedding.

Landing gear noise of four-wheel bogies could be reduced by tilting the bogie with respect to the mean-flow-direction (Fig 27), (Ref 25).

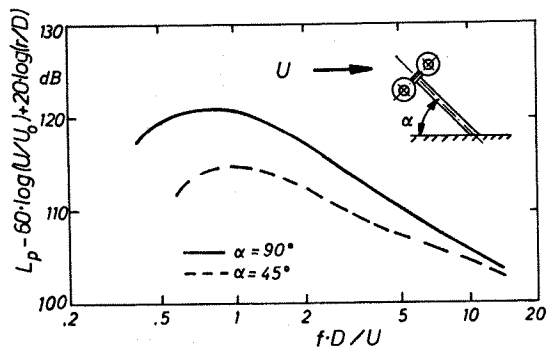


Figure 27 Effect of Tilting Four-wheel Bogie with Respect to the Mean-Flow-direction on Radiated Sound

Thus, the Boeing 747 main-landing-gears - which are tilted during landing approach - should cause less aerodynamic noise. Accordingly arranging landing gears behind each other in the streamwise direction, as might be necessary for large transport aircraft, should be bad practice.

Finally, the wheel-well - if it were a source of (low-frequency) discrete frequency noise - could be shaped as to prevent periodic oscillations to occur. Heller and Bliss (Ref 39) for example demonstrated the feasibility of a slanted trailing edge for the suppression of tonal cavity-noise over a large frequency range.

It must be admitted that all these techniques for the reduction of airframe noise are in a fairly rudimentary conceptual stage. If any of them has been demonstrated, it was through model tests only, where the

scaling effect due to Reynolds-stresses has not at all been clarified. Furthermore, relevant efforts are not pressed very hard at present, since the basic understanding of airframe noise aeroacoustic phenomena is a more urgent problem, and airframe noise reduction is "only" the next step.

## 6. Future Research Needs

Unquestionably, total-aircraft noise studies should be abandoned, unless they serve to check the results of component-studies. Indeed, the authors are of the opinion, that emphasis must be put on studying, preferably through full-scale experiments or - if not feasible - through model-experiments, aerodynamic noise generation from aircraft-components (wings, flaps, slats, landing gears/wheel-well-configurations, but not isolated empty wheel-wells) and their constituents (struts, stringers, actuators, wheel-well doors, cavities). Only through a basic analytical and physical understanding of the aeroacoustic source mechanisms pertinent to aircraft components, and - most importantly - to their aerodynamic and acoustic interaction will the accuracy of prediction schemes be furthered, and the basis provided for the next step of lowering airframe noise below present levels. It is quite significant, that along these lines several major aircraft companies and research institutes are presently conducting or preparing flight-experiments with gliders where both steady-state and unsteady aerodynamic parameters on the wings, in particular wing trailing-edges, are determined and put in relation to ground observed acoustic signatures. In this context there is a particular need of information on surface pressure fluctuation and correlation characteristics on both the pressure- and suction-side of the wings and/or flaps and slats, most desirably on realistic powered aircraft (flown, however, at idle power or with engines off). These very important full-scale and flyover noise measurements need to be supplemented through carefully designed tests in aeroacoustic wind tunnels of the open-jet type. Here a direct source/receiver signal correlation is feasible, providing information on the primary (airframe noise) radiating areas on, say, a wing, a flap, a landing gear etc. Inherent new extremely low noise, low turbulence wind tunnels need to be made available for airframe noise studies.

As far as basic mechanisms is concerned, vortex-noise, edge-noise and turbulent-surface flow noise in-depth analytical and experimental studies are required. Scaling-effects need to be clarified to improve confidence in extrapolating model - test results to the full-scale situation. Likewise - for purposes of flight data acquisition and reduction the understanding of atmospheric and ground reflection effects on sound propagation must be furthered, as well as flight and wind tunnel data acquisition instrumentation be continually improved together with relevant computational procedures.

TABLE I TEST AIRCRAFT FOR AIRFRAME NOISE STUDIES

No	Year	Author(s)	Reference	Aircraft
1	1970	Gibbs, Healy	40	Douglas DC-3
2	1970	Smith, Paxon, Talmadge	7	Libelle Schweizer 2-32 } Gliders Schweizer 2-33 }
3	1970	Healy	3	Prue 2 (Glider) Convair 240 Douglas DC-3 Aero-Commander Shrike Cessna 150
4	1972	NASA Flight Res. Center	-	Aero Commander
5	1973	Gibson	4	C-5A Galaxy
6	1974	Putnam, Lasagna, White	8	JetStar Aero Commander CV-990 Boeing 747
7	1974	Burley	5	F 106 B
8	1975	Munson	41	McDonnell Douglas DC-10
9	1975	Fethney	9	Handley-Page HP 115 Hawker-Siddeley HS 125 British Aircraft Corp. BAC 1-11 Vickers VC-10
10	1976	Cheeseman	41	Chipmunk
11	1977	Bauer, Munson	42	McDonnell Douglas DC9-31
12	1977	Chaussonnet	43	Airbus A-300
13	1977	Dobrzynski, Heller	25 35 38	SB-10 (Glider) Cirrus (Glider) McDonnell Douglas DC-10
14	1977	Grünwald	44	VFW 614
15	1978	Revell	45	Y 12 C

TABLE II OVERALL AIRFRAME NOISE PREDICTION  
- EMPIRICAL RELATIONSHIPS -

No	Author(s)	Year	Ref.	Basic Equation (as presented by Author): Overall Sound Pressure Level is proportional to	Expressed in terms of Air- craft-Speed, Wing-geometric Parameters and Flight-Alt.	Basic Pro- portionality of Overall Sound Pres- sure
1	Healy	1974	3	$\propto 10 \log \left[ \left( \frac{\sin^2 \theta}{r^2} \right) \left( \frac{U^6 S}{AR^4} \right) \right]$	$\propto 10 \log \left[ \frac{U^6 \bar{c}^5}{r^2 1^3} \right]$	$\propto \frac{U^6 S}{AR^4}$
2	Gibson	1974	4	$\propto 10 \log \left[ \left( \frac{U^4}{r^2} \right) \left( \frac{W}{c_L} \right) \left( \frac{\bar{c}}{1} \right) \left( \frac{P_O}{T} \right) \right]$	$\propto 10 \log \left[ \frac{U^6 \bar{c}^2}{r^2} \right]$	$\propto \frac{U^6 S}{AR}$
3	Hardin et al (on the Basis of Healy-Ref4.)	1974	6	$\propto 10 \log \left[ \left( \frac{U^{4.93}}{r^{1.62}} \right) \left( \frac{g \cdot 72}{AR^{2.06}} \right) \right]$	with rounded exp. $\propto 10 \log \left[ \frac{U^5 \bar{c}^3}{r^2 1} \right]$	$\propto \frac{U^5 S^{3/4}}{AR^2}$
4	Putnam, Lasagna, White	1974	8	$\propto 10 \log \left[ \frac{U^5 W}{r^2} \right]$	$\propto 10 \log \left[ \frac{U^7 \bar{c} 1}{r^2} \right]$	$\propto U^7 S$

where  $\bullet W \approx L = \frac{1}{2} \rho c_L \cdot U^2 \cdot S$

$\bullet S = 1 \cdot \bar{c}$

$\bullet AR = \frac{1}{\bar{c}}$

TABLE III AIRCRAFT COMPONENT AND RELEVANT AEROACOUSTIC MECHANISM

Aircraft Component Aero- acoustic Mechanism	Wing	Slat	Flap	Landing Gear	Wheel- well	Wheel- well Doors	Fuse- lage
Direct Turbulent Boundary Layer Radiation	•						•
Lift and Drag Force Fluctuations Due to Turbulent Inflow			•	•			
Lift and Drag Force Fluctuations Due to Turbulent (Wake) Shedding Processes	•	•	•	•		•	
(Free-)Shear Layer Oscillations and Resonant Cavity Response					•		



List of Symbols

$a_0$	m/s	speed of sound	$t$	m	wing thickness maximum
$A$	$m^2$	correlation area	$T$	K	static temperature
$AR$	-	aspect ratio	$U$	m/s	free-stream velocity, flight speed
$c_L$	-	lift coefficient	$U_C$	m/s	convection velocity
$\bar{C}$	m	mean wing chord	$U_O$	m/s	reference speed
$D$	m	wheel-diameter	$U_\infty$	m/s	free-stream velocity, flight speed
$f$	Hz	frequency	$V$	m/s	velocity
$f_{\text{limit}}$	Hz	limiting frequency	$V$	$m^3$	eddy volume
$f_{\text{max}}$	Hz	maximum frequency	$W$	N	weight
$\Delta f$	Hz	frequency bandwidth	$x$	-	coordinate - streamwise direction
$F(\omega)$	N	(fluctuating) force	$\Delta x$	m	sensor separation
$h$	m	flight altitude	$y$	-	coordinate - lateral direction
$I$	Watt/ $m^2$	sound intensity	$Y$	m	wing trailing edge length
$k$	radians/m	wave-number	$\alpha$	-	turbulence intensity
$l$	m	linear source dimension, eddy length scale, wing span	$\gamma$	-	coherence
$l_x$	m	streamwise correlation length	$\delta^*$	m	displacement thickness
$l_y$	m	lateral correlation length	$\eta$	degree	flap angle
$L_p$	dB	sound pressure level	$\theta$	degree	angle observer point and surface plane
$n$	-	number of sources	$\rho_0$	$kg/m^3$	fluid density
OASPL	dB	overall sound pressure level	$\omega$	radians/s	circular frequency
$P_F(f)$	$N/m^2$	farfield RMS (sound) pressure	$\pi_0(\omega)$	Watt	sound power of dipole source
$P_O$	$N/m^2$	static pressure	<u>Abbreviations:</u>		
$P_S(f)$	$N/m^2$	surface RMS (fluctuating) pressure	NLG	nose landing gear	
$q_\infty$	$N/m^2$	free-stream dynamic pressure	CMLG	center main landing gear	
$r$	m	distance, flight altitude, distance source to observer	RMLG	right main landing gear	
$r_O$	m	distance eddy-system from edge	<u>Acknowledgements</u>		
$S$	$m^2$	wing surface area	The authors gratefully acknowledge the help of Burkhard Gehlhar, Elisabeth Rade- macher and Helga Brunner in preparing this manuscript.		
$S_w$	$m^2$	wing surface area			

### References

1. Joint DOT-NASA Civil Aviation Research and Development (CARD) Policy Study. - DOT TST-10-5 and NASA SP-266, March 1971.
2. Kleuters, W. und Hölscher, H. "Durchführbarkeitsstudie zur Herabsetzung des EPNL durch Verwendung von akustisch modifizierten Triebwerksgondeln für das Triebwerk GE/CF 6-50". MBB-Interner Untersuchungsbericht 2090, 1975.
3. Healy, G.J. "Measurement and Analysis of Aircraft Far-Field Aerodynamic Noise". NASA CR-2377, Dec. 1974.
4. Gibson, J.S. "Nonengine Aerodynamic Noise Investigation of a Large Aircraft". NASA CR-2378, 1974.
5. Burley, R. R. "Suppressor Nozzle and Airframe Noise Measurements During Flyover of a Modified F-106B Aircraft with Underwing Nacelles". ASME Paper 74-WA/Aero-1, Nov. 1974.
6. Hardin, J. C., Fratello, D. J., Hayden, R. E., Kadman, Y., Africk, S. "Prediction of Airframe Noise". NASA TN D-7821, Febr. 1975.
7. Smith, D. L., Paxson, R. P, Talmadge, R. D. and Hotz, E. R. "Measurement of the Radiated Noise from Sailplanes". AFFDL-TM-70-3-FDDA, U.S. Air Force, July 1970.
8. Putnam, T. W., Lasagna, P. L. and White, K. C. "Measurements and Analysis of Aircraft Noise". AIAA Paper No. 75-510, March 1975.
9. Fethney, P. "An Experimental Study of Airframe Self-Noise". AIAA Paper 75-511, March 1975.
10. Fink, M. R. "Airframe Noise Prediction Method". FAA-RD-77-29, 1977.
11. Revell, J. D., Healy, D. J. and Gibson, J. S. "Methods for the Prediction of Airframe Aerodynamic Noise". AIAA Paper No. 75-539, March 1975.
12. Hayden, R. E., Kadman, Y., Bliss, D. and Africk, S. "Diagnostic Calculation of Airframe Radiated Noise". AIAA Paper No. 75-485, 1975.
13. Lighthill, M. J. "On Sound Generated Aerodynamically". Pt. I, General Theory, Proc. Roy. Soc., Vol. A 221, pp. 564-587, 1952.  
Pt. II, "Turbulence as a Source of Sound", Proc. Roy. Soc., Vol. A 222, pp. 1-32, 1954.
14. Curle, N. "The Influence of Solid Boundaries Upon Aerodynamic Sound". Proc. Roy. Soc., Vol. A 231, pp. 505-514, 1955.
15. Phillips, O. M. "On the Aerodynamic Surface Sound from a Plane Turbulent Boundary Layer". Proc. Roy. Soc. Lond. A 234, 327-335, 1956.
16. Powell, A. "On the Aerodynamic Noise of a Rigid Flat Plate Moving at Zero Incidence". JASA, Vol. 31, No. 12, pp. 1649-1653, 1959.
17. Vecchio, E. A. and Wiley, C. A. "Noise Radiated from a Turbulent Boundary Layer". J. Acoust. Soc. Am. 53, 596-601, 1973.
18. Tam, C.K.W. "Intensity, Spectrum, and Directivity of Turbulent Boundary Layer Noise". J. Acoust. Soc. Am. 57, 25-34, 1975.
19. Pan, Y.S. "Noise Radiation from Turbulent Flows over Compliant Surfaces". AIAA Paper No. 75-507, 1975.
20. Lotsch, H.K.V., "Fluid Dynamic Generation of Sound in a Plane Turbulent Boundary Layer". Rockwell Report C71-927/401.
21. Ffowcs-Williams, J.E. and Hall, L.H. "Aerodynamic Sound Generation by Turbulent Flow in the Vicinity of a Scattering Half Plane". J. Fluid Mech. Vol. 40, pp. 657-670, March 1970.
22. Hayden, R. E. "Noise from Interaction of Flow with Rigid Surfaces: A Review of Current Status of Prediction Techniques". BBN Rep. No. 2276, also NASA CR-2126, 1972.
23. Morse, P. M. and Ingard, K. U. "Theoretical Acoustic". McGraw-Hill, New York, 1968.
24. Hayden, R. E., Fox, H. L. and Chanaud, R. C. "Some Factors Influencing Radiation of Sound from Flow Interaction with Edges of Finite Surfaces". NASA CR-145073, 1976.
25. Heller, H. H. and Dobrzynski, W. M. "Unsteady Surface Pressure Characteristics on Aircraft Components and Farfield Radiated Airframe Noise". AIAA Paper 1295, AIAA 4th Aeroacoustics Conference, October 3-5, 1977.
26. Hahn, M. "Turbulent Boundary-Layer Surface-Pressure Fluctuations near an Airfoil Trailing Edge". AIAA Paper No. 76-335, San Diego, California (1976).
27. Panton, R. L. "Theoretical and Flight Test Study of Pressure Fluctuations under a Turbulent Boundary Layer", Part 2: "Flight Test Study". NASA CR-140448.

28. Schloemer, H. H. "Effects of Pressure Gradients on Turbulent-Boundary-Layer Wall-Pressure Fluctuations". J. Acoust. Soc. Am., Vol. 42, No. 1, 93-113 (1967).
29. Bull, M. K. "Properties of the Fluctuating Wall-Pressure Field of a Turbulent Boundary Layer". AGARD Report 455, Paris (1963).
30. Bhat, W. V. "Flight Test Measurements of Exterior Turbulent Boundary Layer Pressure Fluctuations on Boeing Model 737 Airplane". J. Sound Vib. (1971), Vol. 14 (4), 439-457 (1971).
31. Corcos, G. M. "Resolution of Pressure in Turbulence". J. Acoust. Soc. Am., Vol. 35, No. 2, 192-199 (1963).
32. Hersh, A. S., Putnam, T. W., Lasagna, P. L. and Burcham, F. W. jr. "Semi-Empirical Airframe Noise Prediction Model". AIAA Paper No. 76-527, July 1976.
33. Bliss, D. and Hayden, R. "Landing Gear and Cavity Noise Prediction". NASA CR-2714, 1975.
34. Heller, H. and Widnall, S. "Sound Radiation from Rigid Flow - Spoilers Correlated with Fluctuating Forces". J.A.S.A. 47, 924-936 (Pf.2) 1970.
35. Dobrzynski, W. M., Heller, H. H. "Are Wheel-well Related Aeroacoustic Sources of any Significance in Airframe Noise?". AIAA Paper No. 77-1270, Atlanta, Georgia (1977).
36. Block, P. J. W. "An Experimental Investigation of Airframe Component Interference Noise". AIAA Paper 77-56 AIAA 15th Aerospace Sciences Meeting Jan. 1977.
37. Fink, M. R. United Technologies Research Center, East Hartford, Ct, USA. Private Communication.
38. Heller, H. H., Dobrzynski, W. M. "Sound Radiation from Aircraft Wheel-well/Landing Gear Configurations". AIAA Paper No. 76-552, Palo Alto, California (1976).
39. Heller, H. H., and Bliss, D. B. "The Physical Mechanism of Flow Induced Pressure Fluctuations in Cavities and Concepts for Their Suppression". AIAA Paper No. 75-491, 1975 and US Airforce Rep., AFFDL-TR-74-133.
40. Gibbs, J. and Healy, G. "Noise from a Gliding DC-3". Report LR 23328, Lockheed Company, 1970.
41. Munson, A. "Modeling Approach to Non-propulsive Noise". AIAA Paper 76-525, 1976.
42. Bauer, A. and Munson, A. "Airframe Noise of the DC-9-31". Report MDC J4582 Douglas Aircraft Co., 1977.
43. Chaussonet, M. "Noise from Airbus Flyovers". Paper No. 14, GARTEur-5 Specialist Meeting on "Airframe Noise" 1976.
44. Grünwald, B. "Airframe Noise Related Studies on VFW 614". Paper No. 15, GARTEur-5 Specialist Meeting on Airframe Noise, 1976.
45. Revell, J. Lockheed-California, Burbank, Ca; USA. Private Communication.
46. Filler, L. "Swept Edge to Reduce the Noise Generated by Turbulent Flow Over the Edge". J.A.S.A. Vol. 59, No. 3, 1976.
47. Hayden, R. and Scharton, T. "A Preliminary Evaluation of Noise Reduction Potential for Upper Blown Flap". BBN Report No. 2478, 1972.
48. Hayden, R., Kadman, Y. and Chanaud, R. "A Study of the Variable Impedance Surface Concept as a Means for Reducing Noise from Jet Interaction with Developed Lift-Augmenting Flaps". BBN Report No. 2399, 1972.
49. Sallett, D. "Splitter Plate for Prevention of Vortex Shedding Behind Finite Circular Cylinders in Uniform Cross-Flow". Naval Ordnance Lab. NOLTR 69-31, 1967.